Journal of Thermal Analysis and Calorimetry (2018) 132:1833–1844
https://doi.org/10.1007/s10973-018-7084-3

Non-isothermal crystallization and oxygen permeability of PP/PLA/EVOH ternary blends

Functions of EVOH

Mohammad Amini[1] · Hassan Ebadi-Dehaghani[1]

Received: 30 April 2017 / Accepted: 15 February 2018 / Published online: 26 February 2018

Abstract
Casting films of polypropylene (PP), poly(lactic acid) (PLA) and ethylene vinyl alcohol copolymer (EVOH) ternary blends having different compositions were prepared. The thermal properties in correlation to the oxygen permeability and mechanical properties of the films were investigated. The morphology of the blends, before and after the film extrusion process was investigated. The SEM images of casted films show a great laminar morphology development in the machine direction. The effects of EVOH and compatibilizer on the relative changes in the crystallization behavior, i.e., melting peak crystallization (X_m%) and degree of crystallization (X_c) are considered. While the compatibilization facilitated the crystallization of PP, it had reverse effect on EVOH crystallization. There is an increase in the X_m% as well as X_c% of EVOH in ternary blend with an increase in EVOH content. The permeability to oxygen was decreased with an increase in EVOH content and compatibilization led to improvement in barrier properties. The crystallinity degree of EVOH revealed to have a greater effect on barrier and mechanical properties as compared to that of PP. Finally, the study of the interaction parameters using Nishi and Wang theory confirmed an effective interaction between the components.

Keywords PP/PLA/EVOH · Ternary blends · Thermal properties · Microstructure · Oxygen permeability

Introduction

Use of multicomponent blends having two or more functions to solve the problems of packaging industries is of great importance [1, 2]. Because of ease of the mass transfer in amorphous regions compared to that of crystal lattices, the thermal properties of ternary blends, especially the crystallinity issue, are of great importance [3]. The controlling of gas permeation in the packaging films has a strong relationship with the crystallinity degree as well as the size of the crystals. Several studies have been widely reported about the crystallization behavior of PLA [4–8]. For instance, the effects of talc on the kinetics and isothermal crystallization behaviors of polylactide/poly(butylene adipate-*co*-terephthalate) (PBAT) blend films have been considered by Phetwarotai et al. [9]. Their results revealed that the presence of PBAT and talc in the films led to an increment of crystallization rate of PLA via a synergistic effect under isothermal crystallization conditions. The crystallization has been reported to impact the structure and oxygen permeability of poly(ethylene oxide)/clay nanocomposite [10]. Komatsuka et al. [11] reported that as the crystallinity in a polymer membrane increases, gas permeability decreases. Their results showed that the size and distribution of free volume in the crystalline PLA blend membrane were different from those in other crystalline polymer membrane. The aging and change in crystallinity were reported to have a significant effect on permeability results elsewhere [12].

The environmental problems lead many recent researches to use biodegradable material blended with commercial polymers, such as polypropylene (PP) [4, 13–15]. Poly(lactic acid) (PLA) gaining of reusable resources has been widely commercialized due to biodegradability. The effects of clay

✉ Hassan Ebadi-Dehaghani
ebadi@iaush.ac.ir

[1] Department of Chemical Engineering, Shahreza Branch, Islamic Azad University, Shahreza, Iran

type and composition on the thermal properties of PP/PLA blends were investigated in our previous work [4]. Moreover, the oxygen permeability determination of the PP/PLA/clay nanocomposites along with a molecular dynamics simulation for prediction of diffusion was carried out elsewhere [16]. Investigations on oxygen gas permeability in PP/PLA/clay nanocomposite films revealed that the permeation is highly dependent on blend composition, clay loading and state of clay dispersion governed by compatibilization. The blending of PP and PLA led to a decrease in the oxygen permeability, and incorporation of clay led to a greater improvement. EVOH copolymer, as a leader in barrier property to nonpolar gases of air, can create a proper hydrocarbon permeation resistance and excellent oxygen barrier properties due to its superior gas barrier property and high oil resistance [17, 18]. EVOH has attracted much attraction for its good barrier property and has been used in binary and ternary blends [17, 19, 20]. The problem of such blends is the lack of biodegradability. The aim of this work is to use biodegradable components in combination with PP and to improve the thermal properties and the oxygen permeability of the PP/PLA blends, consequently. This will be carried out using EVOH as a high-performance oxygen barrier polymer in order to have an advanced green blend for modified atmosphere packaging (MAP) applications.

Theoretical background

According to Flory–Huggins theory [21], the free energy of mixing (ΔG_{mix}) for two polymers and also polymer–polymer interaction parameter χ_{12} can be used as important criteria for prediction of compatibility or miscibility in polymer blends. The free energy of mixing consists of three main contributions: the combinatorial entropy of mixing, the exchange interactions and the free volume contribution. Thermodynamics also predicts that the decrease in chemical potential of the crystalline polymer, due to the presence of the miscible amorphous polymer, leads to a decrease in the melting point. Nishi and Wang [22] have modeled this based on the Flory–Huggins theory to calculate of polymer–polymer interaction parameter χ_{12}. Blend melting points are frequently used to estimate the value of the polymer–polymer interactions at T^0_{mB}.

$$-\left[\frac{\Delta H^0_f V_1}{RV_2}\left(\frac{1}{T^0_{mB}}-\frac{1}{T^0_m}\right)\right]=\chi_{12}(1-\Phi_2)^2 \quad (1)$$

where T^0_{mB} and T^0_m are the equilibrium melting points of the crystallizable component in the blend and pure state, respectively, R is the universal gas constant, V_i is the molar volume of the respective component, ΔH^0_f is the heat of fusion per mole of repeating unit and Φ_2 is the volume fraction of second component in the blend.

Experimental

Materials

Polypropylene (PP) was C30S grade (Maroon Petrochemical Co., Iran), with the density of 0.9 g cm^{-3} and melt flow index (230 °C/2.16 kg) of 6 g $(10\ min)^{-1}$. Ethylene vinyl alcohol copolymer (EVOH) was F171B grade (EVAL Co., Belgium) containing 32 mol% ethylene with the density of 1.18 g cm^{-3} and melt flow index (190 °C/2.16 kg) of 1.8 g $(10\ min)^{-1}$. PLA (4043D grade) was purchased from Nature Works (USA). It had a density of 1.24 g cm^{-3} and weight average molecular weight of 100,000 g mol^{-1}. PP-g-MA, a graft copolymer of propylene and maleic anhydride (MA), was 20093 grade (Priex Co., the Netherland), as a reactive compatibilizer. It had a melt flow index of 12 g $(10\ min)^{-1}$ (190 °C/2.16 kg) and density of 0.94 g cm^{-3}.

Material processing

All of the materials were dried in an oven at 80 °C overnight before melt extrusion. Next the components were dry-blended and processed in a co-rotating twin-screw extruder (LTE 26-32 Model, Labtech Engineering Co. Ltd., Thailand). Different compositions were prepared according to Table 1, and the 75/25 and 25/75 compositions were selected in order to consider the effect of PP-g-MA compatibilizer. The mixing process was carried out at a rotor speed of 100 rpm. The melt strands were cooled in a water bath at the die exit and were pelletized and dried. A cooled strand of each sample was cut at the die exit for morphology study. The film processing was carried out using a Brabender film casting extrusion instrument (KE, Brabender® GmbH & Co., Germany). In order to consider the effect of film casting, the compression molded films were also prepared using a press (20 MT Mini Lab, Labtech

Table 1 Compositions of the samples

Sample code	Components	Composition
a	(PP/PLA 75/25)/EVOH/PP-g-MAH	100/0/0
b	(PP/PLA 75/25)/EVOH/PP-g-MAH	9010/0
c	(PP/PLA 75/25)/EVOH/PP-g-MAH	75/25/0
d	(PP/PLA 75/25)/EVOH/PP-g-MAH	75/25/3
e	(PP/PLA 75/25)/EVOH/PP-g-MAH	75/25/5
f	(PP/PLA 75/25)/EVOH/PP-g-MAH	50/50/0
g	(PP/PLA 75/25)/EVOH/PP-g-MAH	25/75/0
h	(PP/PLA 75/25)/EVOH/PP-g-MAH	25/75/3
i	(PP/PLA 75/25)/EVOH/PP-g-MAH	25/75/5
j	(PP/PLA 75/25)/EVOH/PP-g-MAH	10/90/0

Engineering Co. Ltd., Thailand). For each sample, an equal weight was preheated at 180 °C for 30 s and pressed under 15 MPa pressure for 10 s in a sheet mold, followed by quenching at room temperature, to obtain flat films for the study. The materials were dried in the oven at 80 °C for 12 h before any film processing. In order to eliminate the thermal history, the same procedure was applied so that the thermal history of the blends and that of neat polymers would remain similar.

Characterization

Scanning electron microscopy (SEM)

SEM was used to characterize the morphology of the blends. The mentioned strand of each sample, as well as the film samples after proper drying, was cryofractured in liquid nitrogen at − 160 °C. Then the PLA phase was etched using ethylamine solvent. They were then sputter coated with 3 nm of platinum prior to examination and observed in a SEM (S360 Model, Cambridge Instruments Co., UK). SEM images were analyzed using image processing software. Equations 2–5 are used for calculation of volume ($\bar{R}_V$) and number ($\bar{R}_n$) average radii and polydispersity of the particles (PD) [16]. In order to do so, 200 particles were selected randomly to measure the parameters.

$$\bar{R}_n = \frac{\sum n_i R_i}{\sum n_i} \quad (2)$$

$$\bar{R}_w = \frac{\sum n_i R_i^2}{\sum n_i R_i} \quad (3)$$

$$\bar{R}_V = \frac{\sum n_i R_i^4}{\sum n_i R_i^3} \quad (4)$$

$$PD = \frac{\bar{R}_V}{\bar{R}_n} \quad (5)$$

Differential scanning calorimetry (DSC)

A Mettler DSC (STAR^e SW 10.00) was used to study the degree of crystallinity (X_c) of the specimens. About 5 mg of each sample was scanned in a cycle of heating–cooling–heating from −20 to 200 °C at 10 K min^{-1}. In this study, the cooling and second heating scans were used in order to determine the crystallization enthalpy (ΔH_c), cold crystallization enthalpy (ΔH_{cc}) and melting enthalpy (ΔH_m). The X_c of samples was calculated using the following equation [4, 16]:

$$X_c = \frac{\Delta H}{\Delta H_m^0 \cdot [1 - (\text{wt.\% dispersed phase}/100)]} \times 100 \quad (6)$$

here $\Delta H = \Delta H_c$ for cooling curves, i.e., the crystallization enthalpy of the sample, or $\Delta H = \Delta H_m - \Delta H_{cc}$ for second heating curves, ΔH_m is the melting enthalpy of the sample and ΔH_{cc} is the cold crystallization enthalpy of the sample and ΔH_m^0 is the melting enthalpy of the 100% crystalline of each component (201.1 J g^{-1} for PP [23], 157.8 J g^{-1} for EVOH [24] and 93.0 J g^{-1} for PLA [25]) and wt.% is the total weight percentage of the dispersed components [4, 25].

Oxygen permeability

A gas permeability tester (Coesfeld, GDP-C, Germany) was used to determination of the permeability to oxygen. This instrument determines the permeability of dry gases through thin sheets and films using the manometric method. This is determined by the evaluation of the increase in pressure in the previously evacuated volume at the bottom chamber of the test specimen, versus cm^3 · m^{-2} day^{-1} bar^{-1}. During the test period, the change in pressure is recorded by an external computer. The average values of at least three measurements were reported.

Mechanical properties

The tensile testing was performed on a tensile tester (Zwick/Roell, Germany) according to the ASTM D882 standard test method at room temperature. For all samples, the crosshead speed was 50 mm min^{-1} and the average values of five measurements were reported.

Results and discussion

Morphology

The final properties of polymer blends depend on the extent of dispersion and distribution of the dispersed phase particles within the matrix, strongly. Thus, it is vital to consider the sizes of the particles and their distribution in the blends in order to interpret the test results. The morphology of the blends, before and after film extrusion process is shown in the SEM micrographs of Figs. 1 and 2, respectively. These images were analyzed using the image analysis software. The measured R_n, R_v and PD values, using Eqs. 2–5, are shown in Table 2. The PD values show that the mixing extruder has created a uniform dispersion of discrete spherical domains within the matrix, efficiently. The domain sizes of the dispersed phase, i.e., PLA and EVOH droplet sizes, in the PP/PLA-rich ternary blends (90/10 and 75/25) have less values as compared to the PLA-rich ones (25/75 and 10/90). It is due to the higher

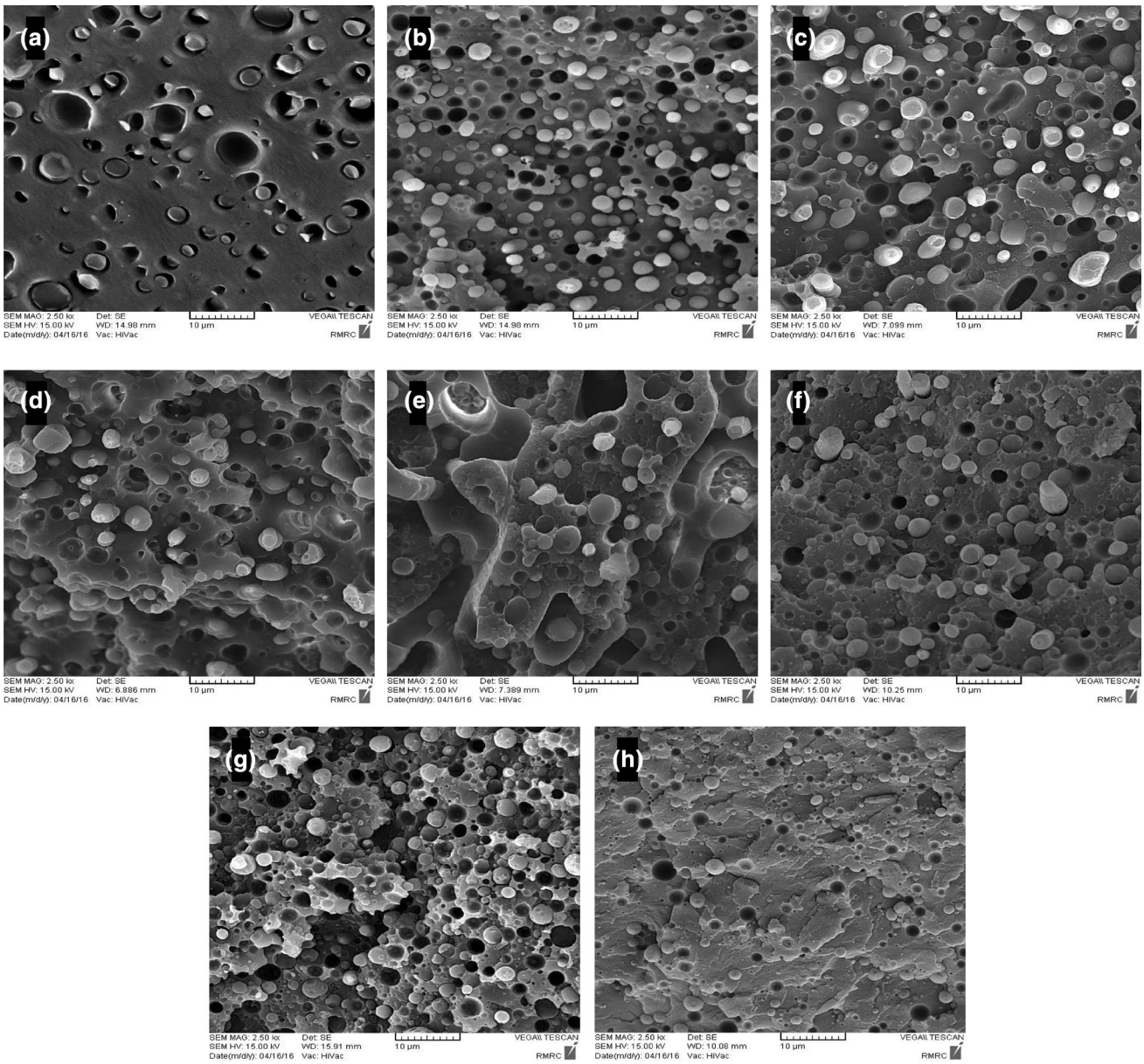

Fig. 1 SEM micrographs of the PP/PLA(75/25)/EVOH/compatibilizer samples before film casting process: **a** 100/0/0, **b** 90/10/0, **c** 75/25/0, **d** 75/25/5, **e** 50/50/0, **f** 25/75/0, **g** 25/75/5, **h** 10/90/0

viscosity of the PP component as the major phase compared to those for PLA and EVOH; this is a significant factor determining the domain size of dispersed phase [26]. The higher viscosity of PP result in a viscosities ratio greater than 1 ($\eta_{PP}/\eta_{PLA} > 1$ and $\eta_{PP}/\eta_{EVOH} > 1$), creating a fined droplet morphology. Moreover, the lower modulus values of PLA [26] and EVOH [27] compared to those for PP is another reason. The similar values of polydispersity of droplet size are also corresponded to the close elasticity of PLA and EVOH as the minor phase. It is suggested that this factor causes to a similar deformation of EVOH and PLA droplets with imposing shear stress within the extruder, leading to a similar polydispersity of the droplet size. The results in Table 2 show the relative decrease in the domain size of the PLA dispersed phase with incorporation of EVOH into the formulation. It seems that the PP-g-MA had a ignorable effect on the blends' morphology of this system, as compared to EVOH. The maximum values of R_n and R_v are seen for 50/50 composition, and again, there is a decrease in domain size as exceed than 50% of EVOH.

Another notable issue in this system is the morphology development in the cast film process. The SEM images of casted films (Fig. 2) show a laminar morphology development more in machine direction (MD). This laminar morphology can improve barrier properties. The film casting process via flat die is not as effective as biaxial

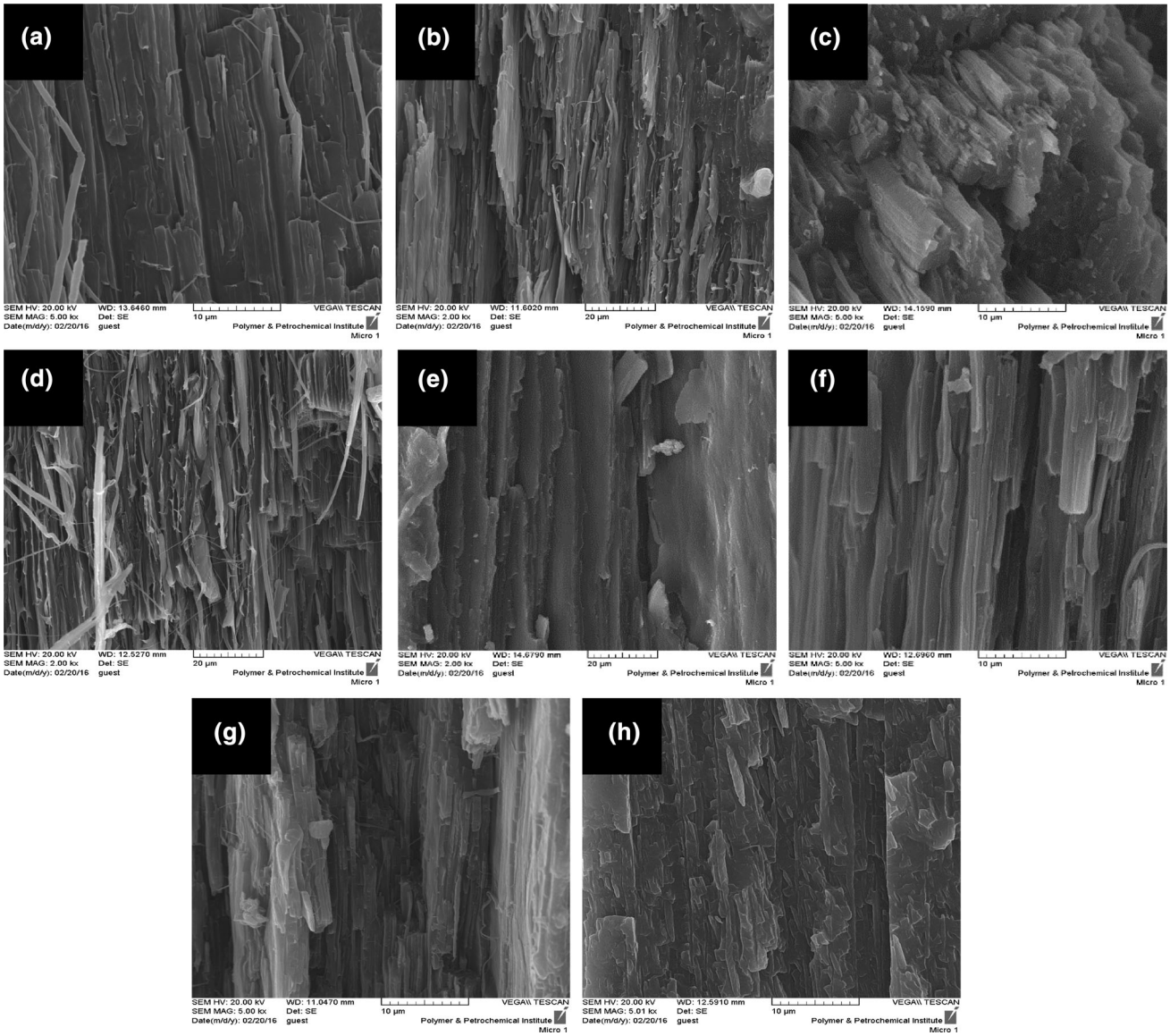

Fig. 2 Effect of film casting process on the morphology of the PP/EVOH (75/25)/PLA/compatibilizer samples: **a** 100/0/0, **b** 90/10/0, **c** 75/25/0, **d** 75/25/5, **e** 50/50/0, **f** 25/75/0, **g** 25/75/5, **h** 10/90/0

stretching for enhancing barrier properties. This is due to the lack of molecular orientation in the transverse direction (TD), resulting in a laminar structure of the dispersed domains with a low area [28].

Thermal analysis results

The effects of EVOH and compatibilizer on the relative changes in the crystallization behavior, i.e., degree of crystallization (X_c) are considered in this section. Figures 3 and 4 show the curves of all samples, and the summary of the results is presented in Table 3a and b.

The curves in Fig. 3 show the thermal properties of the blends' components. The second heating DSC analyses show no glass transition and no cold crystallization temperature for PP and PP/PLA 75/25 blend in the investigated temperature range (Fig. 3a), but the endothermic peak of melting is at 164 and 163.5 °C, respectively. The EVOH component shows a glass transition at 60.6 °C, no cold crystallization and the melting point of 180.8 °C. The DSC cooling curves of PP and EVOH (Fig. 3b), having narrow exothermic peaks with a maximum at 116 and 161.4 °C, respectively, are the main peaks due to the crystallization of PP and EVOH that also appeared in the PP/PLA and (PP/PLA)/EVOH blends. In the case of PLA, the second heating curve shows a glass transition at 60.7 °C. Moreover, there is a cold crystallization temperature at 121 °C and the melting peak is at 152.7 °C [4]. While the cold

Table 2 Quantitative values obtained from SEM micrographs

Sample code	Components	Composition	R_n/μm		R_V/μm		PD	
			PLA phase	EVOH phase	PLA phase	EVOH phase	PLA phase	EVOH phase
a	PP/PLA (75/25)/EVOH	100/0	0.54	–	0.81	–	1.52	–
b	PP/PLA (75/25)/EVOH	90/10	0.79	1.03	0.99	1.17	1.17	1.14
c	PP/PLA (75/25)/EVOH	75/25	0.99	1.19	1.12	1.29	1.07	1.07
e	PP/PLA(75/25)/EVOH/ Comp.	75/25/5	1.10	1.25	1.26	1.45	1.14	1.08
f	PP/PLA (75/25)/EVOH	50/50	1.16	1.35	1.34	1.59	1.14	1.17
g	PP/PLA (75/25)/EVOH	25/75	1.26	1.58	1.40	1.88	1.20	1.20
i	PP/PLA(75/25)/EVOH/ Comp.	25/75/5	1.43	1.64	1.61	1.92	1.12	1.17
j	PP/PLA(75/25)/EVOH	10/90	1.54	1.87	2.53	3.33	1.65	1.78

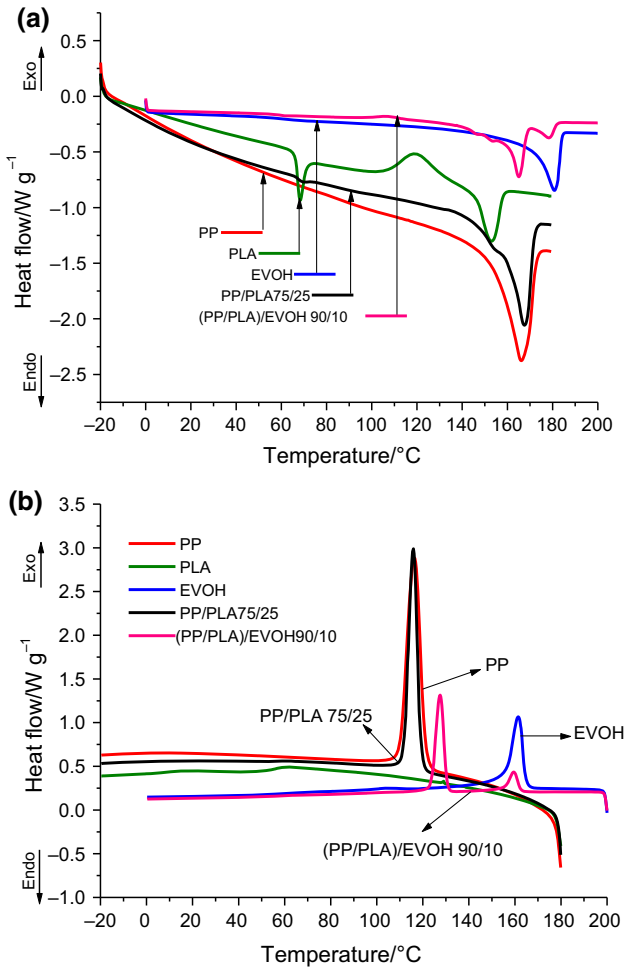

Fig. 3 DSC curves of the blends' components as compared to the 90/10 blend; **a** second heating, **b** cooling

crystallization can be seen for PLA, it is not seen in the binary and ternary blends, suggesting that PP and EVOH could not facilitate the cold crystallization of PLA. As reported in our previous work [4], the DSC cooling curve for PLA is very smooth and no exothermic peak can be observed, indicating that no crystallization occurs during the cooling process at this cooling rate (Fig. 3b).

Blending of PP/PLA and EVOH leads to interesting changes in the thermal behavior of the blends. As shown in Fig. 3a, the second heating curve of the 90/10 blend shows a glass transition corresponding to the PLA phase, and a melting peak at 153.7 °C and a small peak corresponding to the PP and EVOH phases, respectively. There is a decrease in the T_g of the blends with an increase in the EVOH content within the blends. It seems that EVOH can act as a plasticizer, due to its compatibility with PP and PLA components. The effect of compatibilizer on the T_g of the 75/25 blend is opposite of 25/75 one. While the compatibilizer in the 75/25 blend decreases the T_g, it increases the T_g of the 25/75 blend, implying the increase in interaction.

There is an increase in the T_m of EVOH in ternary blend with an increase in EVOH content, while the T_m of PP has no significant change in the ternary blend. This are attributed to the interactions between the EVOH and other components which interrupt the crystallization of EVOH [29]. The ΔH_m values of the PP and EVOH components normalized to their contents as well as the X_m% are reported in Table 3. As shown, the X_m% of PP and EVOH are in competition, i.e., there is a decrease in X_m% value of PP with an increase in EVOH content and increase in X_m% of EVOH. Interestingly, except for 50/50 composition, the sum of two X_m% is approximately a constant value of around 51–55, similar to those for pure PP and EVOH, respectively.

The cooling DSC curve shows a narrow exothermic peak at 125.0 °C and a broad and small peak at 156.4 °C

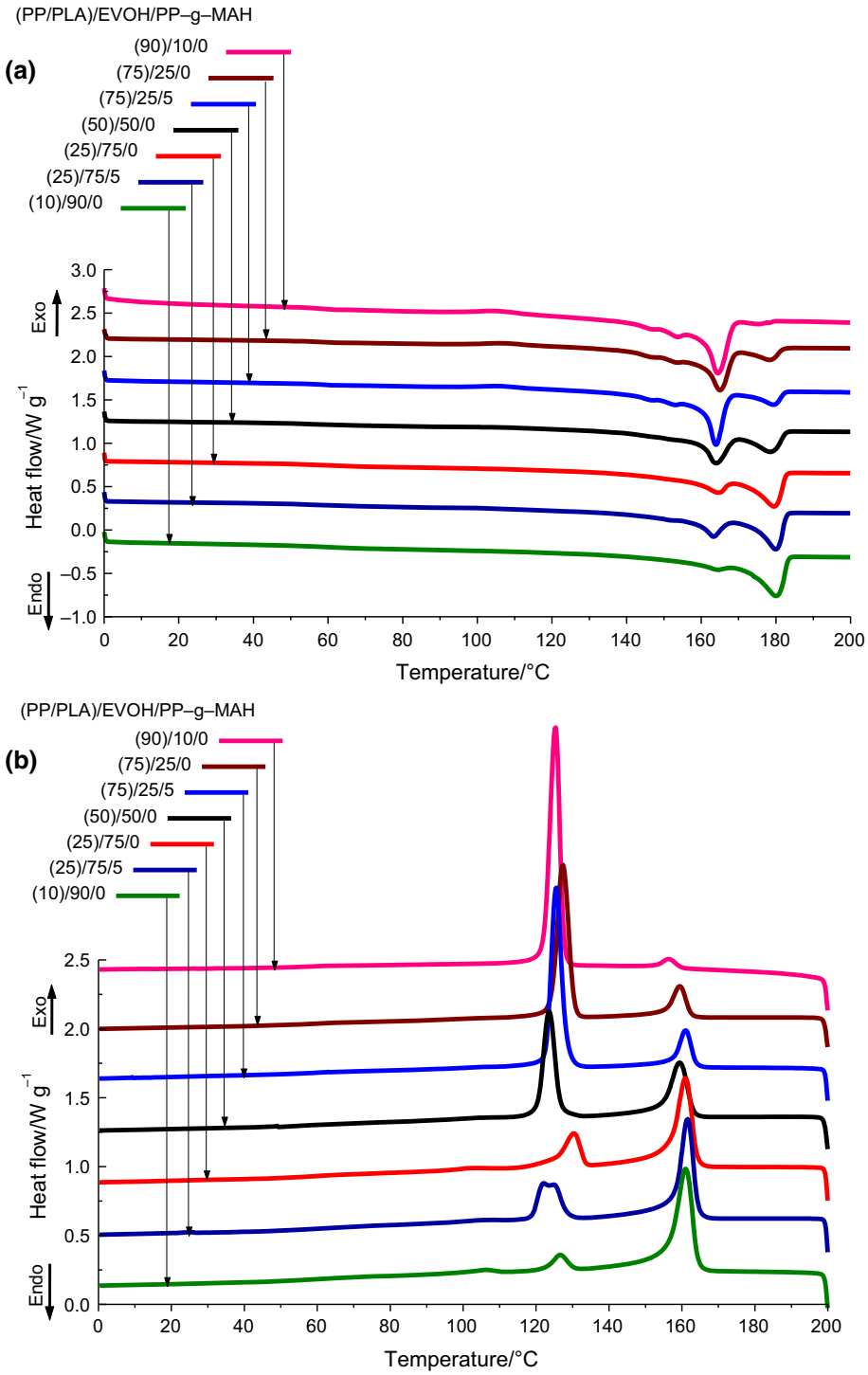

Fig. 4 DSC curves of the blends; **a** second heating, **b** cooling

corresponding to the PP and EVOH phases, respectively (Fig. 3b). Similar to that seen for X_m%, these two peaks have an interesting behavior with changing the composition. They are in competition; as the EVOH content increases, the height of the corresponding crystallization peak increases, and the width decreases and shifts to the higher temperatures. A glance at the T_c values of PP and EVOH shows that the T_c value of it has decreased to the lower temperature, implying that the compatibilization facilitates the crystallization of PP. Conversely, the T_c value of EVOH has increased with addition of compatibilizer, having reverse effect on the EVOH crystallization. A notable point is the effect of compatibilizer on the crystallinity degree of the PP and EVOH. While the

Table 3 DSC analysis of the samples at cooling/heating rate of 10 K min^{-1}: (a) second heating, (b) cooling

Samples	T_g/°C	T_{cc}/°C	ΔH_{cc}/J g^{-1}	X_{cc}/%	T_m/°C			ΔH_m/J g^{-1}		X_m/%	
					PP	PLA	EVOH	PP	EVOH	PP	EVOH
(a) Second heating											
Pure PP	–	–	–	–	164.2	–	–	101.9	–	51.0	–
Pure PLA	60.7	121.1	15.5	16.7	–	152.7	–	–	26.7	–	28.7
PP/PLA 75/25	–	–	–	–	163.5	–	–	88.3	–	51.0	–
PP/PLA (75/25)/EVOH 90/10	60.5	–	–	–	164.4	153.7	175.5	87.6	1.3	43.5	8.1
PP/PLA (75/25)/EVOH 75/25	60.4	–	–	–	165.1	152.9	178.5	61.7	7.9	30.7	20.0
PP/PLA(75/25)/EVOH/C 75/25/5	59.7	–	–	–	164.0	152.8	179.4	64.8	9.2	32.2	23.4
PP/PLA (75/25)/EVOH 50/50	59.6	–	–	–	164.0	152.5	178.5	76.3	22.6	37.9	28.7
PP/PLA (75/25)/EVOH 25/75	58.1	–	–	–	164.9	–	179.4	47.6	38.6	23.7	32.6
PP/PLA(75/25)/EVOH/C 25/75/5	59.3	–	–	–	163.5	151.9	179.8	55.4	39.3	27.5	33.2
PP/PLA (75/25)/EVOH 10/90	58.1	–	–	–	164.6	–	180.0	35.1	47.9	17.4	33.8
Pure EVOH	60.6	–	–	–	–	–	180.8	–	86.5	–	54.8

Samples	T_c/°C		ΔH_c/J g^{-1}		X_c/%	
	PP	EVOH	PP	EVOH	PP	EVOH
(b) Cooling						
Pure PP	116.4		100.5		50.0	
Pure PLA	128.7		7.5		8.1	
PP/PLA (75/25)/EVOH 100/0	115.7	–	71.6	–	47	–
PP/PLA (75/25)/EVOH 90/10	125.3	156.4	71.9	3.3	53.0	20.7
PP/PLA (75/25)/EVOH 75/25	127.5	159.4	56.6	14.7	50.0	37.4
PP/PLA(75/25)/EVOH/C 75/25/5	125.5	161.0	59.2	13.6	52.3	34.5
PP/PLA (75/25)/EVOH 50/50	123.5	159.5	35.8	32.2	47.5	40.8
PP/PLA (75/25)/EVOH 25/75	130.4	161.1	17.6	48.9	46.7	41.4
PP/PLA(75/25)/EVOH/C 25/75/5	122.1	161.7	21.7	48.3	57.4	40.8
PP/PLA (75/25)/EVOH 10/90	126.41	161.2	6.3	60.1	44.6	42.3
Pure EVOH	–	161.4	–	74.5	–	47.2

compatibilizer could increase the crystallinity degree of PP in the both PP/PLA-rich and EVOH-rich blends, it has reverse effect on that for EVOH. This is due to the lack of polar groups in the PP component, affecting by addition of compatibilizer.

In order to use the Nishi and Wang theory, the EVOH was assumed as the crystallizable component and the effect of PLA was ignored. Other assumptions are the PP/PLA 75/25 blend as the first component, having the volume fraction of Φ_1, and EVOH as the second component, having the volume fraction of Φ_2. For use of the theory, T^0_{mB} and T^0_m are the equilibrium melting points of the EVOH component in the blend and pure state, respectively, ΔH^0_f is the heat of fusion of EVOH. Moreover, the T_m values at the rate of DSC are assumed to be equilibrium values. The interaction parameters χ_{12} using Eq. 1 for different compositions were calculated and are presented in Table 4. In order to use Eq. 1, the parameter values are as follows:

$\Delta H^0_f = 157.8\,J\,g^{-1}$, $V_1 = 48.8\,cm^3\,mol^{-1}$,
$V_2 = 34.4\,cm^3\,mol^{-1}$[25] and
R is the universal gas constant $\left(8.314\,J\,mol^{-1}\,K^{-1}\right)$.

As shown, the interaction parameters are negative for all of the compositions except for 90% of EVOH. This is due to the good interactions between the matrix segments and EVOH. The depression of T_m and χ_{12} values with increasing EVOH content implies that EVOH is compatible with other components. The increase in the EVOH content up to 75% leads to decrease in χ_{12} value and exceeding 75% has converse effect.

Table 4 Values of Φ_{EVOH}, T_m^0 and χ_{12} of the blends

Components	Composition	Φ_{EVOH}	T_m^0/°C	χ_{12}
PP/PLA (75/25)/EVOH	100/0	0	–	–
PP/PLA (75/25)/EVOH	90/10	0.080	175.5	− 0.00068
PP/PLA (75/25)/EVOH	75/25	0.213	178.5	− 0.00029
PP/PLA(75/25)/EVOH/C	75/25/5	0.209	179.4	− 0.00009
PP/PLA (75/25)/EVOH	50/50	0.448	178.5	− 0.00058
PP/PLA (75/25)/EVOH	25/75	0.709	179.4	− 0.00069
PP/PLA(75/25)/EVOH/C	75/25/5	0.702	179.8	− 0.00007
PP/PLA(75/25)/EVOH	10/90	0.880	180.0	0.00136
PP/PLA(75/25)/EVOH	0/100	1	180.8	–

Permeability of the films

The oxygen permeability values of the samples at ambient conditions are shown in Table 5. As seen, oxygen permeability is initially reduced with increasing compatibilizer content. This result may be explained by the fact that the addition of compatibilizer up to a certain level results in thinning of EVOH layers due to efficient stress transfer from the matrix (PP) to the dispersed phase (EVOH and PLA) during film stretching process.

Properties of a semicrystalline polymer are related not only to the X_m% and X_c% values, but also to the crystalline characteristics, such as the size and the perfection of the crystals. The good barrier properties of EVOH component is strongly attributed to the degree of crystallinity and the presence of impermeable crystalline regions. The presence of crystalline regions can lead to reduction in gas permeability by creating a tortuous diffusive path for penetrant molecules. Moreover, the presence of crystalline phase within a polymer lead to a decrease in required space for occurrence of the solution phenomenon. Cerrada et al. and different researchers reported that slowly cooling in EVOH creates orthorhombic structure for all copolymer compositions, resulting in effective barrier properties [30]. The thin-film casting process has such condition, due to the low thickness of film and effective cooling rate.

As shown, the PP/PLA film has a lower barrier property as compared to the ternary blends because the oxygen molecules can diffuse through the probable micro-voids formed at the interface during stretching process [4]. This is due to poor interfacial adhesion between PP and PLA. Meanwhile, it seems that the EVOH has multifunctional effects on the permeability. First of all, its role as an intrinsic barrier material can be denoted due to its proper micro- and macrostructure, such as high molecular weight, polarity and crystallinity. Second, its role as a compatibilizer; the addition of EVOH, as well as the PP-g-MA compatibilizer, to the PP/PLA immiscible blend prevents coalescence of the dispersed particles during melt flow in two processes, i.e., melt blending and flat film extrusion. Finally, the presence of EVOH beside PP and performing the cast film process has created a high degree of crystallinity, resulting in decrease in oxygen permeability. As shown in Fig. 5, there is a good relationship between the oxygen permeability (Fig. 5a) and crystallinity (Fig. 5b, c) of the samples. Moreover, it is confirmed that while the

Table 5 Oxygen permeability of the sample films at ambient conditions

Samples	Permeability (P)/cm^3 m^{-2} day^{-1} bar^{-1}
PP	349
PP/PLA (75/25)/EVOH 100/0	416
PP/PLA (75/25)/EVOH 90/10	358
PP/PLA (75/25)/EVOH 75/25	323
PP/PLA (75/25)/EVOH/Comp. 75/25/3	278
PP/PLA (75/25)/EVOH/Comp. 75/25/5	221
PP/PLA (75/25)/EVOH 50/50	163
PP/PLA (75/25)/EVOH 25/75	109
PP/PLA (75/25)/EVOH/Comp. 25/75/3	76
PP/PLA (75/25)/EVOH/Comp. 25/75/5	64
PP/PLA (75/25)/EVOH 10/90	45
PP/PLA (75/25)/EVOH 0/100	9
PLA	24

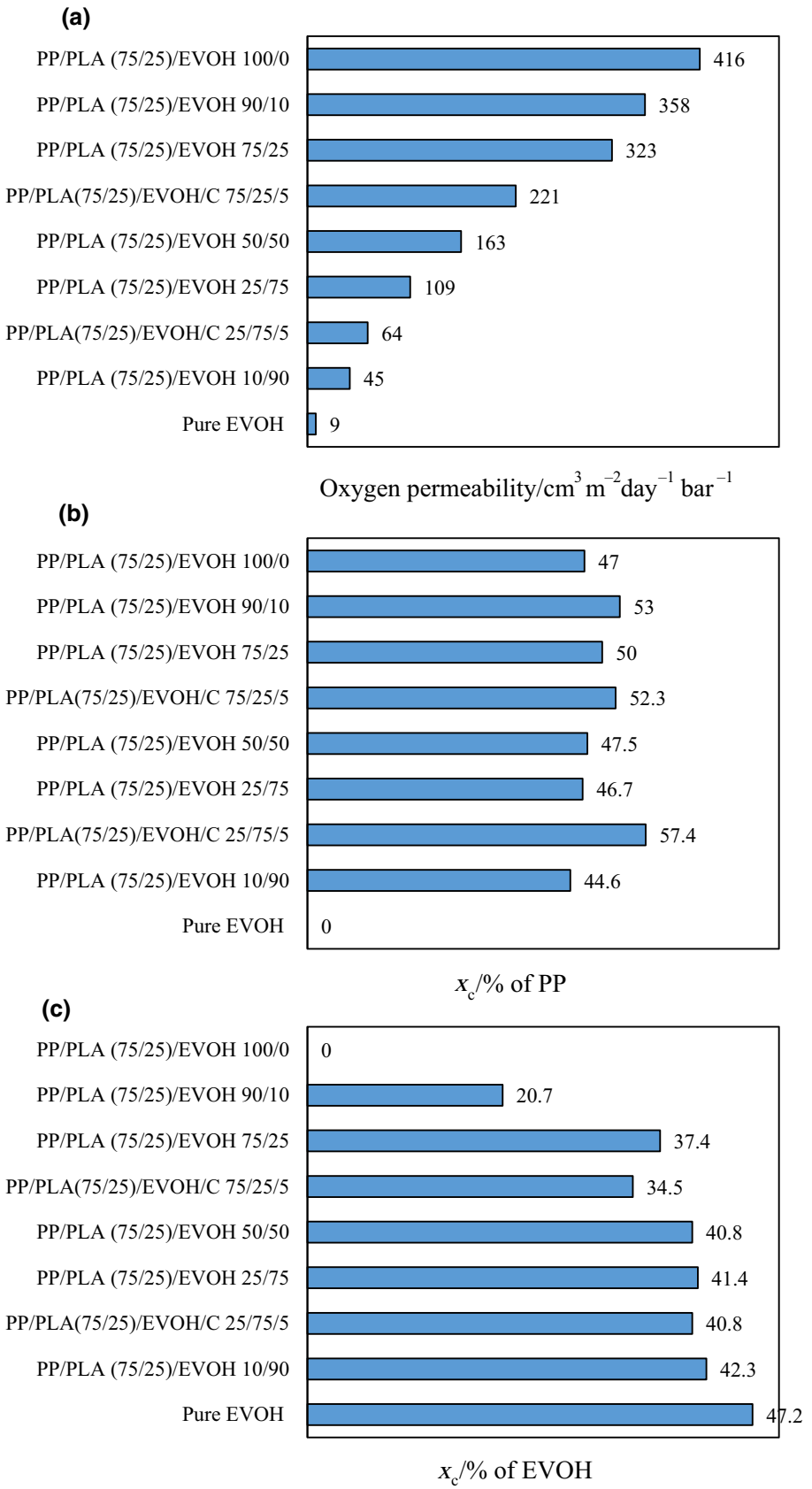

Fig. 5 Graph of permeability values (**a**) as compared to the degree of crystallinity of PP (**b**) and EVOH (**c**)

Table 6 Mechanical properties of the samples of the blends at ambient conditions

Components	Composition	Tensile modulus/MPa	Tensile strength/MPa	Elongation at break/%
PP/PLA (75/25)/EVOH	100/0	343 ± 6.9	6.9 ± 0.1	3.5 ± 0.18
PP/PLA (75/25)/EVOH	90/10	393 ± 5.3	7.5 ± 0.15	2.2 ± 0.02
PP/PLA (75/25)/EVOH	75/25	438 ± 4.6	8.3 ± 0.23	2.7 ± 0.09
PP/PLA(75/25)/EVOH/C	75/25/3	453 ± 5.8	7.2 ± 0.3	2.9 ± 0.09
PP/PLA(75/25)/EVOH/C	75/25/5	485 ± 10.6	7.1 ± 0.38	3.7 ± 0.09
PP/PLA (75/25)/EVOH	50/50	510 ± 9.8	8.4 ± 0.19	3.2 ± 0.1
PP/PLA (75/25)/EVOH	25/75	595 ± 11.7	12.8 ± 0.41	3.8 ± 0.13
PP/PLA(75/25)/EVOH/C	25/75/3	617 ± 13.2	11.2 ± 0.32	5.2 ± 0.11
PP/PLA(75/25)/EVOH/C	75/25/5	643 ± 16.9	10.7 ± 0.46	5.9 ± 0.10
PP/PLA(75/25)/EVOH	10/90	665 ± 14.3	13.2 ± 0.42	4.2 ± 0.13
PP/PLA(75/25)/EVOH	0/100	740 ± 18.1	14.9 ± 0.5	4.8 ± 0.2

crystallinity degree of the both components has synergistic effect on the oxygen barrier properties, the crystallinity degree of EVOH seems to be more important (Fig. 5c).

Mechanical properties of the films

The tensile properties and impact strength of the samples for this series of blends are shown in Table 6. There is an increase in the tensile modulus of the blends with an increase in the EVOH content. This is due to the greater value of the EVOH modulus (740 Mpa) and also its compatibilizing effect as mentioned in the SEM results. Another important factor determining the tensile properties, especially modulus, is the degree of crystallinity. As mentioned above, there is an increase in the crystallinity of the EVOH with an increase in its content, while the crystallinity degree of PP has not such improvement. Therefore, it seems that the crystallinity of EVOH has more significant effect on the modulus and other mechanical properties as compared to that of PP. Change in composition results in similar trends for tensile strength as well as impact strength. Differently, while there is no regular trend for elongation at break, the compatibilizer can increase it to some extent. An important notable point is the maximum impact strength value for the 50/50 composition. Similar results have been reported in our previous work for PP/PLA blends [31]. The image in Fig. 1e shows a co-continuous morphology in this composition. This morphology has been reported to have extraordinary effects on the properties and leads to synergism of properties, such as high modulus and high impact strength in commercial blends. An improvement in the impact strength of the blends with an increase in EVOH content would be expected due to the higher impact strength of EVOH compared to that of PP/PLA blend. However, the experiment values did not match with such expecting results. In other words, there was a maximum in impact strength of the blends up to 50/50 composition, dropped again at greater contents of EVOH. However, addition of PP-g-MA led to an increase due to increase in compatibility between the components. This increase is due to enhancement in interface interaction, affecting the chain motions and frictions between them and resulting in dissipation of imposed energy. The EVOH-rich blend showed significant increase in impact strength compared to that of PP/PLA-rich blend. This is due to toughening effect of PP droplets being at the rubbery plateau at experiment temperature, i.e., 23 °C, in the blend [32]. Hence, it can be stated that when the stress concentration occurs in the PP/PLA-rich blend, the EVOH droplets cannot dissipate the sudden impact energy. Therefore, the imposed energy led to promotion of the cavities at the interface under stress. Therefore, the composition of a blend plays an important role in the impact strength of the blend [31, 33].

Conclusions

Casting films of PP/PLA/EVOH ternary blends having different compositions were prepared. From the laminar morphology development of the dispersed phases, it was concluded that there was effective interaction between the components, especially in the presence of the EVOH. This morphology is one of the responsible factors resulted in decrease in the oxygen permeability. The crystallinity degrees of two crystalline components of the ternary blends, i.e., PP and EVOH, had an interesting relationship, so that the average of their crystallinity remained around 35–45%. The EVOH has multifunctional effects on the properties of the casting films, as an intrinsic barrier material, as compatibilizer and as a high-potential crystalline material, resulting in the decrease in oxygen permeability and increase in mechanical properties. While the compatibilization facilitated the crystallization of PP, it had

reverse effect on EVOH crystallization. Nishi and Wang theory confirmed an effective interaction between the components. The significant increase in the impact strength in the EVOH-rich blends compared to that of PP/PLA-rich ones was due to toughening effect of PP droplets being at the rubbery plateau at experiment temperature. The increase in the crystallinity of EVOH had a greater effect on the modulus and tensile strength, as compared to that for PP.

Acknowledgements The work described in this paper was supported by a grant from the Islamic Azad University, Shahreza branch. The authors gratefully acknowledge the Research Vice Chancellor of Islamic Azad University of Shahreza and his co-workers for their help and assistance.

References

1. Blanco I, Siracusa V. Kinetic study of the thermal and thermo-oxidative degradations of polylactide-modified films for food packaging. J Therm Anal Calorim. 2013;112(3):1171–7.
2. Tham W, Poh B, Ishak ZM, Chow W. Transparent poly(lactic acid)/halloysite nanotube nanocomposites with improved oxygen barrier and antioxidant properties. J Therm Anal Calorim. 2016;126(3):1331–7.
3. Van Krevelen DW, Te Nijenhuis K. Properties of polymers: their correlation with chemical structure; their numerical estimation and prediction from additive group contributions. Amsterdam: Elsevier; 2009.
4. Ebadi-Dehaghani H, Barikani M, Khonakdar HA, Jafari SH. Microstructure and non-isothermal crystallization behavior of PP/PLA/clay hybrid nanocomposites. J Therm Anal Calorim. 2015;121(3):1321–32.
5. Vidović E, Faraguna F, Jukić A. Influence of inorganic fillers on PLA crystallinity and thermal properties. J Therm Anal Calorim. 2016;127(1):371–80.
6. Li H, Lu X, Yang H, Hu J. Non-isothermal crystallization of P(3HB-*co*-4HB)/PLA blends. J Therm Anal Calorim. 2015;122(2):817–29.
7. Phetwarotai W, Aht-Ong D. Nucleated polylactide blend films with nanoprecipitated calcium carbonate and talc. J Therm Anal Calorim. 2017;127(3):2367–81.
8. Ye Q, Huang Z, Hao Y, Wang J, Yang X, Fan X. Kinetic study of thermal degradation of poly(L-lactide) filled with β-zeolite. J Therm Anal Calorim. 2016;124(3):1471–84.
9. Phetwarotai W, Aht-Ong D. Isothermal crystallization behaviors and kinetics of nucleated polylactide/poly(butylene adipate-*co*-terephthalate) blend films with talc. J Therm Anal Calorim. 2016;126(3):1797–808.
10. Wang H, Keum JK, Hiltner A, Baer E. Confined crystallization of PEO in nanolayered films impacting structure and oxygen permeability. Macromolecules. 2009;42(18):7055–66.
11. Komatsuka T, Kusakabe A, Nagai K. Characterization and gas transport properties of poly(lactic acid) blend membranes. Desalination. 2008;234(1):212–20.
12. Huang Y, Paul D. Physical aging of thin glassy polymer films monitored by gas permeability. Polymer. 2004;45(25):8377–93.
13. Sathe SN, Devi S, Rao G, Rao K. Relationship between morphology and mechanical properties of binary and compatibilized ternary blends of polypropylene and nylon 6. J Appl Polym Sci. 1996;61(1):97–107.
14. Sathe SN, Srinivasa Rao G, Rao K, Devi S. The effect of composition on morphological, thermal, and mechanical properties of polypropylene/nylon-6/polypropylene-g-butyl acrylate blends. Polym Eng Sci. 1996;36(19):2443–50.
15. Hassan A, Wahit MU, Chee CY. Mechanical and morphological properties of PP/NR/LLDPE ternary blend—effect of HVA-2. Polym Test. 2003;22(3):281–90.
16. Ebadi-Dehaghani H, Barikani M, Khonakdar HA, Jafari SH, Wagenknecht U, Heinrich G. On O_2 gas permeability of PP/PLA/clay nanocomposites: a molecular dynamic simulation approach. Polym Test. 2015;45:139–51.
17. Wang B, Yang Y, Guo W. Effect of EVOH on the morphology, mechanical and barrier properties of PA6/POE-g-MAH/EVOH ternary blends. Mater Des. 2012;40:185–9.
18. Lagaron JM, Powell AK, Bonner G. Permeation of water, methanol, fuel and alcohol-containing fuels in high-barrier ethylene–vinyl alcohol copolymer. Polym Test. 2001;20(5):569–77.
19. Rastin H, Jafari SH, Saeb MR, Khonakdar HA, Wagenknecht U, Heinrich G. Mechanical, rheological, and thermal behavior assessments in HDPE/PA-6/EVOH ternary blends with variable morphology. J Polym Res. 2014;21(2):1–13.
20. De Petris S, Laurienzo P, Malinconico M, Pracella M, Zendron M. Study of blends of nylon 6 with EVOH and carboxyl-modified EVOH and a preliminary approach to films for packaging applications. J Appl Polym Sci. 1998;68(4):637–48.
21. Sperling LH. Introduction to physical polymer science. Hoboken: Wiley; 2005.
22. Nishi T, Wang T. Melting point depression and kinetic effects of cooling on crystallization in poly(vinylidene fluoride)-poly(-methyl methacrylate) mixtures. Macromolecules. 1975;8(6):909–15.
23. Vakili M, Ebadi-Dehaghani H, Haghshenas-Fard M. Crystallization and thermal conductivity of $CaCO_3$ nanoparticle filled polypropylene. J Macromol Sci Part B. 2011;50(8):1637–45.
24. Oyama HT. Super-tough poly(lactic acid) materials: reactive blending with ethylene copolymer. Polymer. 2009;50(3):747–51.
25. Brandrup J, Immergut EH, Grulke EA, Abe A, Bloch DR. Polymer handbook. New York: Wiley; 1989.
26. Ebadi-Dehaghani H, Khonakdar HA, Barikani M, Jafari SH, Wagenknecht U, Heinrich G. An investigation on compatibilization threshold in the interface of polypropylene/polylactic acid blends using rheological studies. J Vinyl Addit Technol. 2014;22(1):19–28.
27. Ares A, Silva J, Maia JM, Barral L, Abad MJ. Rheomechanical and morphological study of compatibilized PP/EVOH blends. Rheol Acta. 2009;48(9):993–1004.
28. Ebadi H, Yousefi AA, Oromiehie A. Reactive extrusion and barrier properties of PP/PET films. Iran Polym J. 2007;16(10):659–69.
29. Jiang W, Qiao X, Sun K. Mechanical and thermal properties of thermoplastic acetylated starch/poly(ethylene-*co*-vinyl alcohol) blends. Carbohydr Polym. 2006;65(2):139–43.
30. Mokwena KK, Tang J. Ethylene vinyl alcohol: a review of barrier properties for packaging shelf stable foods. Crit Rev Food Sci Nutr. 2012;52(7):640–50.
31. Ebadi-Dehaghani H, Khonakdar HA, Barikani M, Jafari SH. Experimental and theoretical analyses of mechanical properties of PP/PLA/clay nanocomposites. Compos B Eng. 2015;69:133–44.
32. Michler GH, Balta-Calleja FJ. Mechanical properties of polymers based on nanostructure and morphology. Boca Raton: CRC Press; 2016.
33. Utracki LA, Wilkie CA. Polymer blends handbook. Berlin: Springer; 2002.